Carbon Dioxide Capture at Nucleophilic Hydroxide Sites in Oxidation-Resistant Cyclodextrin-Based Metal-Organic Frameworks

Mary E. Zick,[a] Suzi M. Pugh,[b] Jung-Hoon Lee,[c] Alexander C. Forse,[b] Phillip J. Milner[a,*]

[a]Department of Chemistry and Chemical Biology, Cornell University, Ithaca, NY, 14850, United States

[b]Yusuf Hamied Department of Chemistry, University of Cambridge, Cambridge, CB2 1EW, United Kingdom

[c]Computational Science Research Center, Korea Institute of Science and Technology (KIST), Seoul 02792, Republic of Korea

ABSTRACT: Carbon capture and utilization or sequestration (CCUS) from industrial point sources and direct air capture (DAC) are likely necessary to combat global climate change. Reducing the costs of CCUS and DAC requires next-generation sorbents capable of reversible CO_2 capture under realistic conditions. A particular challenge faced by amine-based sorbents—the current leading technology for carbon capture—is poor stability towards O_2, which is present in high partial pressures in most emission streams of interest as well as in air. Sorbents containing oxygen-based nucleophiles, such as hydroxide (OH^-), can reversibly react with CO_2 to form (bi)carbonate (HCO_3^-) species and should display improved oxidative stabilities compared to amine-based materials. Here, we provide gas sorption, spectroscopic, and computational studies supporting that CO_2 chemisorption in γ-cylodextrin-based metal-organic frameworks (CD-MOFs) occurs via HCO_3^- formation at nucleophilic OH^- sites within the framework pores, rather than via previously proposed pathways involving carbonic acid or alkyl carbonate formation. Of the CD-MOFs studied herein, the new framework $KHCO_3$ CD-MOF possesses rapid and high-capacity CO_2 uptake, good thermal, oxidative, and cycling stabilities compared to previously reported materials, and selective CO_2 capture under mixed gas conditions in dynamic breakthrough experiments. Because of its low cost and performance under realistic conditions, $KHCO_3$ CD-MOF is a promising new platform for CCUS. More broadly, our work demonstrates that the encapsulation of reactive OH^- sites within a porous framework represents a potentially general strategy for the design of oxidation-resistant adsorbents for carbon dioxide capture.

INTRODUCTION

Global climate change resulting from the anthropogenic release of greenhouse gases is one of the biggest challenges facing humankind.[1] Carbon dioxide generated as a byproduct of industrial processes accounts for approximately two-thirds of greenhouse gas emissions each year.[1,2] Limiting the rise in average global temperature necessitates carbon capture and utilization or sequestration (CCUS) from industrial point sources.[3] Although CCUS from coal-fired power plants—the current largest source of anthropogenic CO_2 emissions—has received significant attention, other currently unavoidable point sources such natural gas-fired combined cycle (NGCC) power plants, cement manufacturing, and steel production, are increasingly contributing to anthropogenic CO_2 emissions each year.[1,4–7] Direct air capture (DAC) of CO_2 to achieve net-negative emissions will likely be needed to reach climate targets as well.[8,9] Unfortunately, the current costs of CCUS and DAC technologies are likely untenable without significant subsidies.[6,10] Reducing the costs of these technologies to viable levels requires the development of next-generation sorbents capable of reversible CO_2 capture with high CO_2 capacities, fast kinetics, low regeneration energies, and excellent long-term stabilities.

Beyond the criteria outlined above, an important yet often overlooked consideration for new carbon capture sorbents is their robustness towards other reactive components in target gas streams, such as O_2.[4,5] Indeed, O_2 is one of the major components of coal flue gas (4%), NGCC plant emissions (12%), cement kiln off-gas (8%), and air (21%).[4] Although aqueous amine scrubbers, the current best-in-class technologies for CCUS, demonstrate highly selective CO_2 capture,[11] they suffer from significant oxidative degradation upon cycling.[12–15] Additionally, amines are highly corrosive, leading to large regeneration costs and low CO_2 capacities due to their necessary dilution with large volumes of water, ionic liquids, or organic solvents.[16,17] The latter challenges can potentially be overcome by grafting amines to porous solid supports,[4] such as zeolites,[18] silicas,[19] and metal-organic frameworks (MOFs),[20–22] but these materials still frequently suffer from oxidative degradation of the electron-rich amine moieties.[23–30] Oxidative degradation is one of the main challenges currently facing electrochemical CO_2 capture as well.[31] Therefore, overcoming the limitations of current sorbents requires the development of new CO_2 capture chemistries employing nucleophiles with superior oxidative stabilities compared to amines.[32]

Oxygen-based nucleophiles, such as alcohols and oxide, hydroxide, and alkoxide salts, can reversibly react with CO_2 to form (bi)carbonate species and should display improved oxidative stabilities compared to amines due to the higher electronegativity of oxygen.[16,32] Indeed, aqueous solutions of hydroxide salts such as KOH are one of the leading technologies for DAC.[8,9] However, aqueous hydroxide scrubbers suffer from large regeneration energy costs due to the high

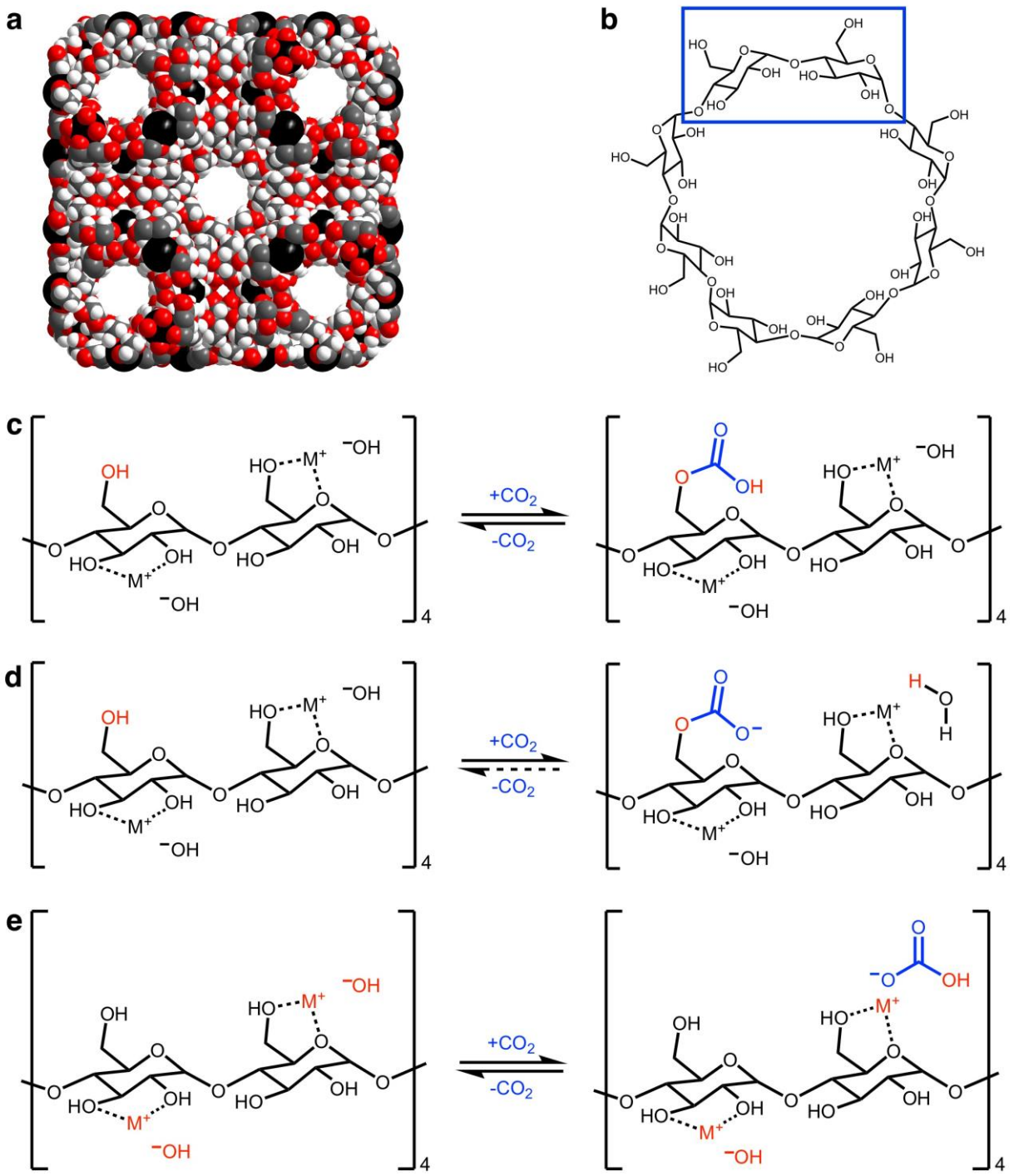

Figure 1. a) Space-filling model of the unit cell of $K_2(OH)_2$(γ-CD) or CD-MOF-1, referred to herein as KOH CD-MOF for consistency, which is composed of γ-cyclodextrin (γ-CD) units linked by K^+ cations with charge-balancing OH^- anions in the pores. The OH^- anions cannot be resolved crystallographically. b) Structure of γ-CD. c) Proposed CO_2 chemisorption pathway involving carbonic acid formation at the primary alcohols of the D-glucopyranose units. d) Proposed CO_2 chemisorption pathway involving alkyl carbonate formation at the primary alcohols of the D-glucopyranose unit, with the concomitant generation of H_2O. e) Proposed CO_2 chemisorption involving (bi)carbonate formation at charge-balancing OH^- sites.

temperatures required to desorb CO_2 from carbonate salts (*e.g.* 900 °C for regeneration of $CaCO_3$).[9,33,34] Additionally, metal oxide and hydroxide salts suffer from sluggish reactivity towards CO_2 in the solid state.[35,36] In contrast to the wide study of amine-functionalized porous solids for CO_2 capture, hydroxide- and alkoxide-functionalized porous solids remain remarkably understudied.[32] This may be due in part to the generally poor stability of traditional solid supports such as mesoporous silicas[37] and MOFs[38,39] towards OH^-. Nonetheless, previous studies have shown that robust azolate MOFs bearing terminal M–OH (M = Zn, Ni, Co) sites can undergo selective and reversible reaction with CO_2 to form metal-bound bicarbonates, akin to the enzyme carbonic anhydrase.[40–44] Similarly, OH^--rich anion exchange resins have been shown to undergo selective CO_2 capture from air via bicarbonate formation.[45] These promising results suggest that porous solids functionalized with oxygen-based nucleophiles merit further study as an alternative to

amine-functionalized materials for CO_2 capture from O_2-containing streams.

An intriguing early example of CO_2 chemisorption in a porous solid lacking amines involves cyclodextrin-based MOFs (CD-MOFs, Figure 1a).[46–54] These frameworks are composed of γ-cyclodextrins (γ-CDs), cyclic oligosaccharides that are mass-produced enzymatically from starch (Figure 1b), linked by alkali metal cations into porous cubic or hexagonal frameworks with charge-balancing anions in the pores.[54] Intriguingly, the cubic structures $K_2(OH)_2$(γ-CD), also known as CD-MOF-1 and referred to herein as KOH CD-MOF, and $Rb_2(OH)_2$(γ-CD), also known as CD-MOF-2 and referred to herein as RbOH CD-MOF, were previously shown to strongly chemisorb CO_2, but the exact pathway remains unclear.[51–54] Three potential mechanisms for CO_2 chemisorption in these materials can be envisioned: carbonic acid formation involving the primary alcohols of the D-glucopyranose units (Figure 1c), alkyl carbonate formation involving the primary alcohols of the D-glucopyranose units and charge-balancing OH^- sites (Figure 1d), and bicarbonate formation via the charge-balancing OH^- sites within the framework pores (Figure 1e). The first mechanism (Figure 1c) is favored by scattered experimental results,[52,53] while the second (Figure 1d) has recently been supported in computational studies.[55] We hypothesize that alkyl carbonate formation at the D-glucopyranose units (Figure 1d) is unlikely due to the general need for countercations derived from organic superbases (*e.g.* guanidinium) to stabilize alkyl carbonates through H-bonding interactions.[56] In addition, this pathway would likely be poorly reversible due to the concomitant formation of free H_2O, akin to the irreversibility of dehydrative urea formation in amine-functionalized silicas.[57] Nonetheless, elucidating the mechanism of CO_2 capture in these and related materials would pave the way for the design of next-generation porous materials bearing nucleophilic oxygen sites for CCUS and DAC.

Herein, we provide gas sorption, spectroscopic, and theoretical evidence supporting that CO_2 chemisorption in both known and new CD-MOFs occurs via HCO_3^- formation at nucleophilic OH^- sites within the framework pores (Figure 1e). In particular, we demonstrate that chemisorption only occurs in frameworks prepared using nucleophilic counteranions (OH^-, HCO_3^-, CO_3^{2-}), and not in frameworks containing non-basic and non-nucleophilic counteranions (OAc^-, OBz^-, Cl^-). Among the CD-MOFs studied herein, the new and inexpensive framework $KHCO_3$ CD-MOF prepared under solvothermal conditions possesses high CO_2 capacities in both volumetric (2.78 mmol/g, 1 bar CO_2, 30 °C) and isobaric (2.09 mmol/g, 1 bar CO_2, 30 °C) measurements. Critically, this material also displays excellent thermal and cycling stabilities compared to all other CD-MOFs, along with selective CO_2 capture under mixed gas conditions in dynamic breakthrough experiments using simulated coal flue gas (15% CO_2 in N_2, 40 °C). Promisingly, $KHCO_3$ CD-MOF also retains its CO_2 capacity after exposure to flowing air for extended periods of time at 40 °C. Owing to its low cost and promising performance, $KHCO_3$ CD-MOF is a potential new platform for carbon capture applications. More broadly, this work demonstrates that the local environment of OH^- sites can be tuned in the solid state to produce oxidatively stable materials capable of reversibly binding CO_2.

RESULTS AND DISCUSSION

Counteranion effects on CO_2 capture. To elucidate the pathway for CO_2 chemisorption in CD-MOFs, we first evaluated the effect of changing the charge-balancing counteranions on CO_2 adsorption in these materials. If the adsorption pathway involves the OH^- sites (Figures 1d–e), then changing the counteranion should have a large effect on the ability of the MOFs to strongly bind CO_2. On the other hand, if the adsorption pathway involves carbonic acid formation at the primary alcohols of the D-glucopyranose units (Figure 1c), then changing the counteranion should not significantly impact CO_2 adsorption. Previous studies have examined the role of the counteranion in CD-MOFs by preparing frameworks using F^- salts,[53] but frameworks prepared using basic F^- salts in water could still contain residual OH^- sites. As such, we elected to prepare K-based CD-MOFs using both nucleophilic (OH^-, HCO_3^-, CO_3^{2-}) and non-basic and non-nucleophilic (OAc^-, Cl^-, OBz^-) counteranions from the corresponding K salts (see Supporting Information or SI Section 2 for details).[58] Initially, we hypothesized that frameworks prepared from (bi)carbonate salts should release CO_2 upon activation to reveal reactive OH^- sites.[40–42] For consistency, frameworks are referred to herein as MX CD-MOFs (M = cation, X = anion) based on the salts used during their preparation.

In contrast to the range of cations that have been used to prepare MOFs from γ-CD,[47] the scope of counteranions that have been incorporated into these materials remains relatively limited. Indeed, only the previously reported KOH and KOBz CD-MOFs could be reliably prepared under the standard vapor diffusion conditions.[53,54,58] The synthesis of CD-MOFs by vapor diffusion also involves long synthesis times (1–3 weeks), limiting the scalability of these materials. Gratifyingly, we have found that new CD-MOFs can be prepared from $KHCO_3$, K_2CO_3, KOAc, and KCl under solvothermal conditions at 120–160 °C using 4:1 MeOH:H_2O as the solvent instead (see SI Section 2 for details). Notably, KOH CD-MOF could be prepared under solvothermal conditions as well (SI Figure S5), but the sample prepared using vapor diffusion exhibited higher CO_2 uptake and thus was employed for all subsequent measurements (SI Figure S121). All prepared frameworks were found to be isostructural to CD-MOF-1 by powder X-ray diffraction (PXRD) and to be similarly porous to CD-MOF-1 as well, with the exception of the framework prepared from KOBz that contains large benzoate anions in the pores. Notably, the presence of non-nucleophilic OAc^- and OBz^- counteranions in the corresponding frameworks were confirmed by both IR spectroscopy (SI Figures S18 and S27, respectively) and ^1H NMR spectroscopy after digestion in D_2O (SI Figures S17 and S26, respectively).[58] Assuming an empirical formula of $K_2(X)_x(OH)_{2-x}$(γ-CD) (X = OAc or OBz), KOAc CD-MOF was determined to contain 82% of the theoretical amount of

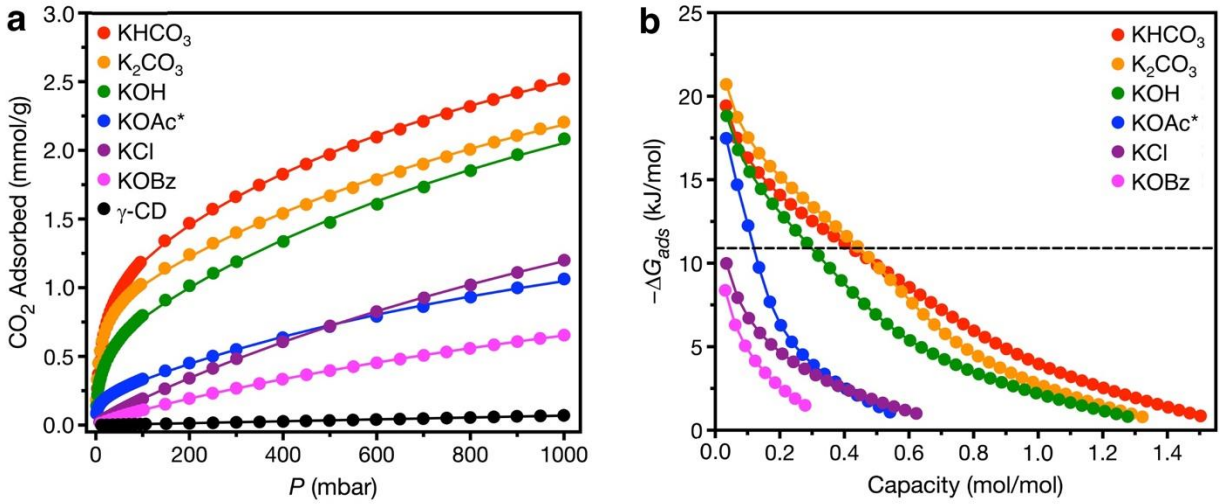

Figure 2. a) CO_2 adsorption isotherms of activated CD-MOFs with different counteranions at 40 °C. Solid lines represent fits to the dual-site Langmuir model. A data point was considered equilibrated when less than 0.01% change in pressure occurred over a 45 s interval. b) Free energies of adsorption ($-\Delta G_{ads}$) for CO_2 adsorption as a function of loading for CD-MOFs with different counteranions at 40 °C. Materials that have $-\Delta G_{ads}$ values above the dashed line at 10.9 kJ/mol can adsorb CO_2 at a 90% capture rate from a coal flue gas stream, as determined using the equation $\Delta G = RT\ln(P/P_0)$ with T = 313 K, P = 15 mbar, and P_0 = 1 bar.[60] *KOAc CD-MOF contains 18% OH^- and 82% OAc^- counteranions, as determined by ^1H NMR (SI Figure S17).

Table 1. CO_2 uptakes and $-\Delta G_{ads}$ values at 40 °C for K-based CD-MOFs with varying counteranions.

MOF	CO_2 uptake at 15 mbar (mmol/g)	CO_2 uptake at 1 bar (mmol/g)	$-\Delta G_{ads}$ at 40 °C (kJ/mol)
KOH CD-MOF	0.42	2.06	18.8
$KHCO_3$ CD-MOF	0.63	2.50	19.4
K_2CO_3 CD-MOF	0.65	2.19	20.7
KOAc CD-MOF	0.19	1.05	17.5
KCl CD-MOF	0.04	1.19	9.99
KOBz CD-MOF	0.02	0.65	8.37

OAc^- sites and KOBz CD-MOF to contain 92% of the theoretical amount of OBz^- sites, with the remainder of charge-balancing anions assumed to be residual OH^- anions that cannot be observed by ^1H NMR spectroscopy. Additionally, the presence of Cl^- throughout KCl CD-MOF was confirmed by energy-dispersive X-ray spectroscopy (EDX, SI Figure S22).

With a range of CD-MOFs bearing different counteranions in hand, we next measured their CO_2 adsorption/desorption isotherms at 30 °C, 40 °C, and 50 °C (Figure 2, see SI Section 3 for details). The 40 °C adsorption isotherms of these CD-MOFs along with a reference sample of commercially available γ-CD are included in Figure 2a. These isotherms confirm that the counteranion in CD-MOFs significantly affects their CO_2 adsorption properties, which is inconsistent with CO_2 adsorption via carbonic acid formation (Figure 1c). For example, $KHCO_3$ (2.50 mmol/g), K_2CO_3 (2.19 mmol/g), and KOH (2.06 mmol/g) CD-MOFs possess significantly higher CO_2 uptakes at 40 °C and 1 bar of CO_2 than the KOAc (1.05 mmol/g), KCl (1.19 mmol/g), and KOBz (0.65 mmol/g) CD-MOF analogues (Table 1). Free γ-CD also showed limited CO_2 uptake under the same conditions (0.07 mmol/g). This is unsurprising because, unlike alkylamines, alcohols generally require the presence of strong base to react with CO_2.[56]

In addition, the adsorption isotherms of $KHCO_3$, K_2CO_3, and KOH CD-MOFs are much steeper in the low-pressure regime than KCl and KOBz CD-MOFs, reflecting their stronger affinity towards CO_2. To achieve >90% capture from a coal flue gas stream (15% CO_2, 1 bar total pressure, 40 °C),[59] a material should possess high uptake at 15 mbar of CO_2 at 40 °C. Indeed, $KHCO_3$ (0.63 mmol/g), K_2CO_3 (0.65 mmol/g), and KOH (0.42 mmol/g) CD-MOFs exhibit higher capacities at 15 mbar of CO_2 and 40 °C than CD-MOFs containing non-nucleophilic counteranions as well (Table 1). Interestingly, KOAc CD-MOF displayed steep uptake until a loading of approximately 0.25 mmol/g (~0.1 mol CO_2/mol MOF), followed by more gradual uptake at higher pressures. This is consistent with the approximately 18% residual OH^- sites in this material, as determined by ^1H NMR spectroscopy (SI Figure S17). Notably, CO_2 uptake was found to be fully reversible in all cases, as confirmed by desorption isotherms collected at every temperature (SI Figures S46, S51, S56, S61, S66, and S71). This finding supports CO_2 capture at the OH^- sites as the dominant pathway (Figure 1e), as alkyl carbonate formation (Figure 1d) would likely be partially irreversible due the gradual loss of concomitantly generated H_2O upon desorption and re-activation.[57]

To gain further insight into the thermodynamics of CO_2 adsorption in CD-MOFs bearing different counteranions, the 30 °C, 40 °C, and 50 °C CO_2 adsorption isotherms were fit to dual-site Langmuir models (Figure 2a, SI Tables S1–6). Using these fits, the heats ($-\Delta H_{ads}$), entropies ($-\Delta S_{ads}$), and free energies of adsorption at 40 °C ($-\Delta G_{ads}$) as a function of uptake were calculated for each material (SI Table S13, see SI Section 3 for details). Consistent with the observations outlined above, the maximum $-\Delta H_{ads}$ values for KOH (55.9 ± 0.5 kJ/mol), $KHCO_3$ (49.5 ± 1.8 kJ/mol), and K_2CO_3 (56.7 ± 2.0 kJ/mol) CD-MOFs are larger in magnitude than those for KOAc (45.3 ± 12 kJ/mol), KCl (36.0 ± 2.7 kJ/mol), and KOBz (44.8 ± 0.1 kJ/mol) CD-MOFs. Although $-\Delta H_{ads}$ values are frequently used to compare the strengths of gas binding in porous solids, these values ignore the contribution of

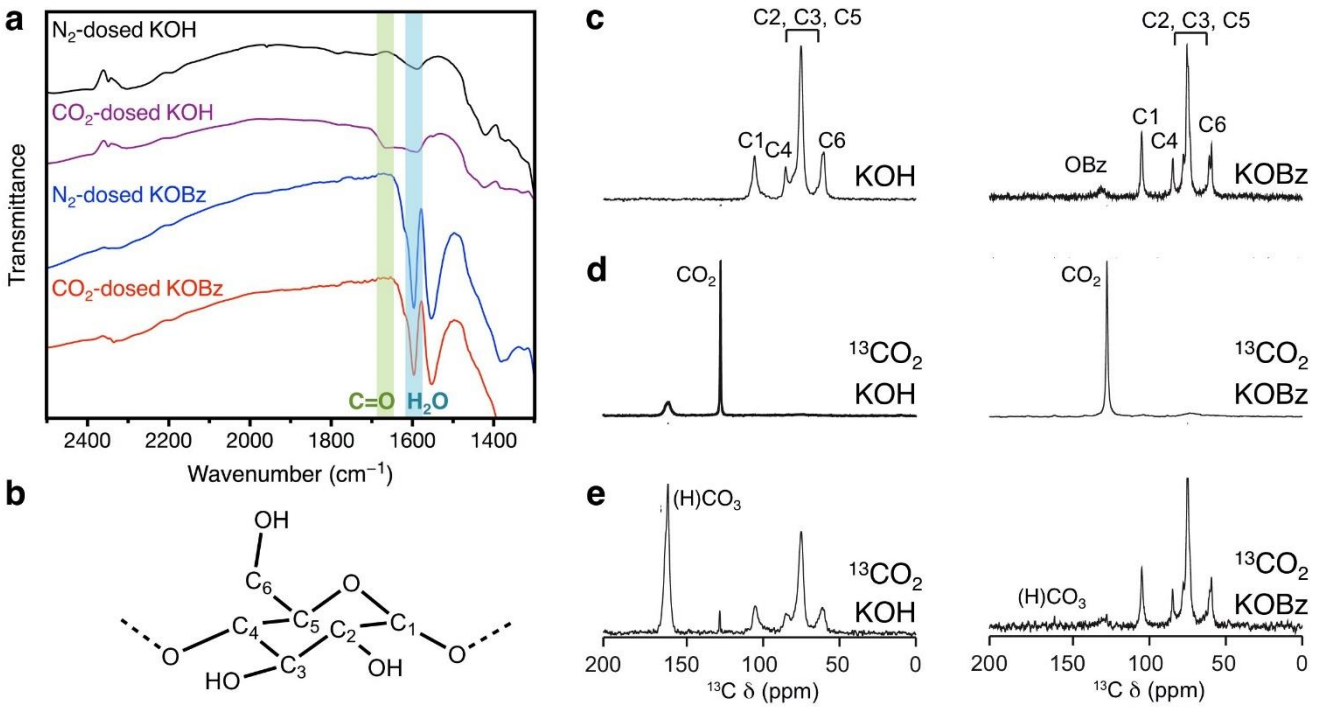

Figure 3. a) TIR spectra of activated KOH CD-MOF and KOBz CD-MOF after dosing with N_2 and with CO_2. The new carbonyl stretch observed in KOH CD-MOF but not in KOBz CD-MOF upon exposure to CO_2 is highlighted in green. The stretch at approximately 1600 cm^{-1} corresponding to permanently bound H_2O observed in all CD-MOF samples is highlighted in blue. b) γ-CD unit with labelled carbons. c) ^1H–^{13}C CP MAS NMR spectra (1 ms contact time) of activated KOH CD-MOF and KOBz CD-MOF. d) ^{13}C MAS SSNMR spectra of KOH CD-MOF and KOBz CD-MOF after dosing with $^{13}CO_2$ gas. e) ^1H–^{13}C CP MAS SSNMR spectra (1 ms contact time) of KOH CD-MOF and KOBz CD-MOF after dosing with $^{13}CO_2$ gas. All SSNMR experiments were carried out at 9.4 T with a spin rate of 15 kHz.

entropic effects on gas adsorption, which can be substantial[60] and correlated with enthalpic effects.[61] For example, while KOBz CD-MOF exhibits a maximum $-\Delta H_{ads}$ value (44.8 ± 0.1 kJ/mol) higher than that of KCl CD-MOF (36.0 ± 2.7 kJ/mol), the CO_2 uptake of KCl CD-MOF is superior. However, the maximum $-\Delta S_{ads}$ value for KOBz CD-MOF is also higher in magnitude (126 ± 0.4 J/mol·K for KOBz vs 87.7 ± 3.5 J/mol·K for KCl). The higher entropic penalty for CO_2 adsorption in KOBz CD-MOF suggests that more structure reorganization occurs upon CO_2 adsorption in this material, potentially due to the large benzoate ions in the pores, which reduces the affinity of this material towards CO_2 compared to KCl CD-MOF. As such, $-\Delta H_{ads}$ values alone do not accurately reflect the thermodynamic differences among CD-MOFs.

Potential enthalpic and entropic differences among CD-MOFs were accounted for by instead comparing $-\Delta G_{ads}$ values as a function of CO_2 loading at 40° C (Figure 2b and Table 1).[61] A comparison of $-\Delta G_{ads}$ values confirms that $KHCO_3$, K_2CO_3, and KOH CD-MOFs exhibit a stronger driving force for CO_2 capture at all loadings compared to the KCl and KOBz CD-MOFs (Figure 2b and Table 1). The higher affinity of $KHCO_3$, K_2CO_3, and KOH CD-MOFs towards CO_2 at low partial pressures makes them better suited for trace CO_2 capture from target streams. For example, these CD-MOFs possess $-\Delta G_{ads}$ values above the dashed line at 10.9 kJ/mol, confirming their suitability for >90% CO_2 capture from a coal flue gas stream.[60] In addition, among CD-MOFs bearing non-nucleophilic counteranions, the trend in $-\Delta G_{ads}$ values is OAc > Cl > OBz, properly reflecting their affinity towards CO_2 in isothermal measurements (Figure 2a). Overall, these gas adsorption data confirm that the counteranion has a critical role in the mechanism of reversible CO_2 chemisorption in CD-MOFs, ruling out CO_2 capture via carbonic acid formation as the dominant pathway (Figure 1c).

Comparing $-\Delta G_{ads}$ values also illuminates the origin of the generally superior CO_2 uptake of $KHCO_3$ CD-MOF and K_2CO_3 CD-MOF compared to KOH CD-MOF. Although all three frameworks possess similar affinities towards CO_2 at low loadings, reflecting the presence of similar binding sites, the strong binding of CO_2 in KOH declines more rapidly at higher loadings, suggesting that it contains fewer accessible OH^- sites. This finding is likely due to the gradual decomposition of KOH CD-MOF during the isothermal measurements, as this material reproducibly changed in color from white to orange and lost crystallinity upon repeated re-activation (SI Figure S103). Remarkably, $KHCO_3$ CD-MOF retained its original color and crystallinity during the collection of CO_2 isotherms (SI Figure S104), reflecting an unexpectedly superior stability compared to the isostructural KOH CD-MOF. This may be due to the different nature of defect sites in these two materials, as KOH CD-MOF is prepared under more basic conditions than $KHCO_3$ CD-MOF.[62]

Mechanistic investigation of CO_2 capture in CD-MOFs. We next carried out spectroscopic and computational studies to investigate the pathway for CO_2 capture in nucleophilic CD-MOFs using KOH and KOBz CD-MOFs as representative materials (Figure 3–4). To confirm that CO_2 chemisorption occurs only in CD-MOFs bearing OH^- sites, transmission infrared (TIR) spectra were collected for activated CD-MOF samples with a range of counteranions dosed with N_2 and with CO_2 (see SI section 4 for details). After exposure

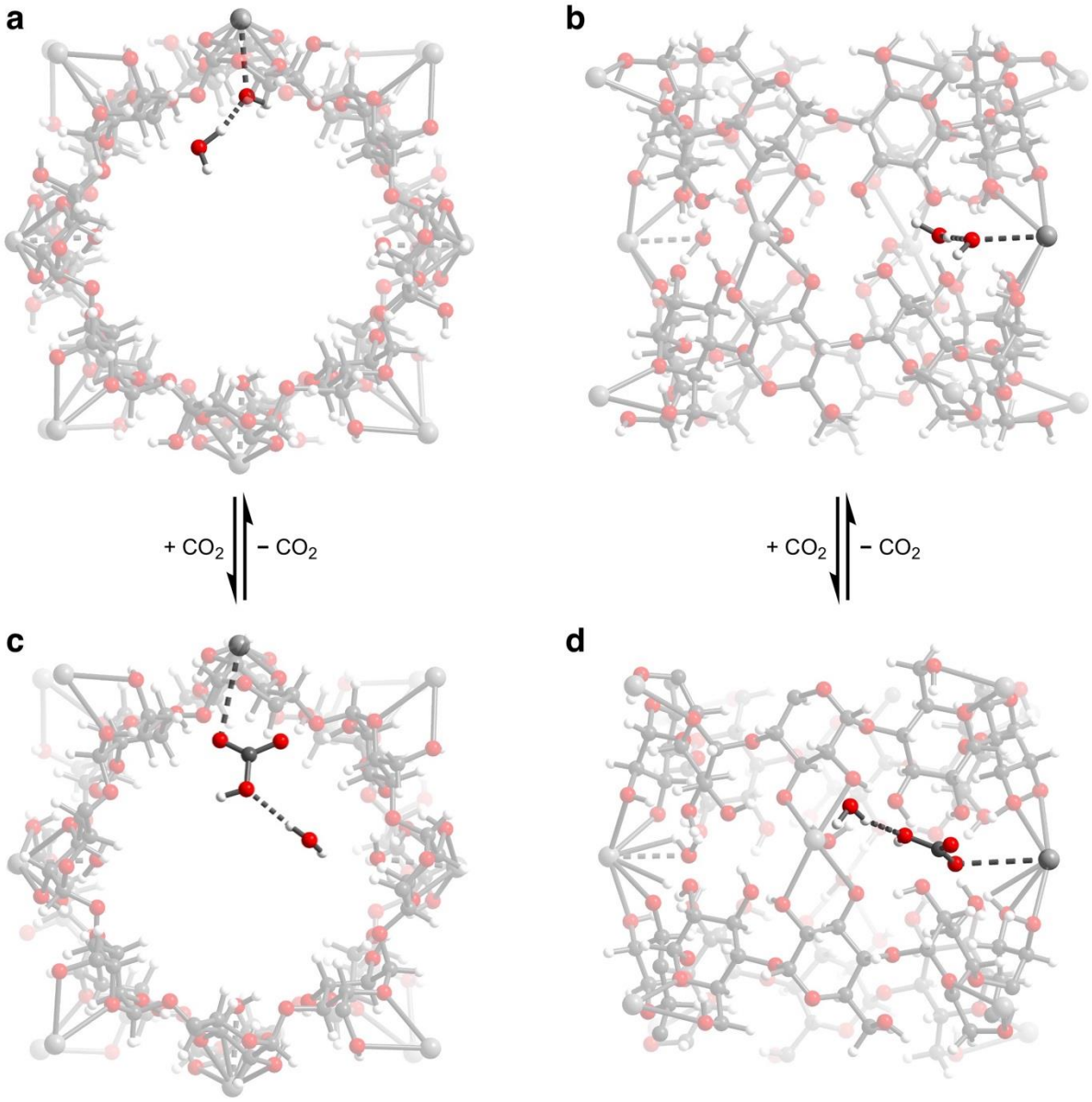

Figure 4. DFT-calculated structures for H_2O-bound KOH CD-MOF a) viewing along *c* and b) viewing along *a*. DFT-calculated structures for the proposed binding mode of CO_2 in the presence of H_2O in KOH CD-MOF via bicarbonate (HCO_3^-) formation c) viewing along *c* and d) viewing along *a*. Gray, white, silver, and red spheres correspond to carbon, hydrogen, potassium, and oxygen atoms, respectively.

to CO_2, a new stretch at 1663 cm^{-1} was observed in the TIR spectrum of KOH CD-MOF (Figure 3a), consistent with the carbonyl stretch of a HCO_3^- species.[63] Similar new stretches were also observed upon dosing activated $KHCO_3$ (SI Figure S106) and K_2CO_3 (SI Figure S107) CD-MOFs with CO_2. In contrast, no new carbonyl stretches were observed upon dosing KOBz (Figure 3a), KCl (SI Figure S112), and KOAc (SI Figure S113) CD-MOFs with CO_2. Consistent with the gas sorption results (Figure 2), these findings suggest that detectable CO_2 chemisorption only occurs in frameworks bearing OH^- sites, further ruling out CO_2 capture via carbonic acid formation (Figure 1c).

To further elucidate the mechanism of CO_2 chemisorption in CD-MOFs, magic angle spinning (MAS) solid-state NMR (SSNMR) spectra of KOH CD-MOF and KOBz CD-MOF were collected before and after dosing with $^{13}CO_2$ gas (Figure 3c–e; see SI Section 6 for details). Both CD-MOFs were treated under the same conditions so that the peak intensities of any newly formed species could be compared directly. Prior to dosing with $^{13}CO_2$, the MAS SSNMR spectra of activated KOH CD-MOF and KOBz CD-MOF are relatively similar, primarily showing resonances ascribed to the γ-CD units (Figure 3b–c). The presence of OBz^- anions in KOBz CD-MOF was confirmed by the observation of an additional broad resonance centered at 128.4 ppm (Figure 3c, right).

After dosing with $^{13}CO_2$ gas, the ^{13}C MAS SSNMR spectra of both materials contains a strong signal at 125.0 ppm assigned to physisorbed $^{13}CO_2$ (Figure 3d). Importantly, the spectrum of $^{13}CO_2$-dosed KOH CD-MOF gas revealed an additional resonance at 159.6 ppm, assigned to a newly formed (H)$^{13}CO_3$ species (Figure 3d, left). This chemical

shift is in line with that assigned to (bi)carbonate species in both molecular and materials systems.[64–66]

Table 2. DFT-calculated energies of adsorption ($-\Delta E_{ads}$) for CO_2 adsorption pathways in KOH CD-MOF and RbOH CD-MOF.

CO_2 Adsorption Pathway	$-\Delta E_{ads}$ without H_2O (kJ/mol)	$-\Delta E_{ads}$ with H_2O (kJ/mol)
HCO_3^- formation (K)	72.0	47.7 (55)[a]
HCO_3^- formation (Rb)	82.1	53.5 (56)[a]
Alkyl carbonate formation (Rb)	51.9	29.5
Physisorption (Rb)	34.8	21.3

[a]Maximum experimental $-\Delta H_{ads}$ determined using the Clausius-Clapeyron equation.

Importantly, the observed chemical shift (159.6 ppm) is closer to that of $KHCO_3$ (161 ppm) than that of K_2CO_3 (168 ppm), supporting its assignment as a HCO_3^- species resulting from reaction at the OH^- sites (Figure 1e).[67] This resonance was not readily observed in the corresponding spectrum of KOBz CD-MOF (Figure 3d, right). After ^1H–^{13}C cross-polarization (CP), which enhances the signals of ^{13}C nuclei near ^1H nuclei (*i.e.*, strengthening MOF resonances over those of physisorbed $^{13}CO_2$), the MAS SSNMR spectrum of $^{13}CO_2$-dosed KOH CD-MOF still contains an intense resonance assigned to a $H^{13}CO_3$ species at 159.6 ppm (Figure 3e, left). The spectrum of KOBz CD-MOF possesses a small resonance at the same chemical shift, which can be ascribed to trace $^{13}CO_2$ chemisorption at the approximately 8% of residual OH^- sites in this material (Figure 3e, right). Due to the large difference in intensity of the newly formed $H^{13}CO_3^-$ resonances in KOH CD-MOF and KOBz CD-MOF upon exposure to $^{13}CO_2$, it can be concluded that the OH^- sites present in the former and lacking in the latter are likely responsible for chemisorptive CO_2 capture.

Van der Waals (vdW)-corrected density functional theory (DFT) calculations were also carried out to probe potential binding modes of CO_2 in KOH CD-MOF and the isostructural RbOH CD-MOF (Figure 4 and Table 2; see SI Section 7 for details). The computed CO_2 binding energy ($-\Delta E_{ads}$) for HCO_3^- formation in KOH CD-MOF is 72.0 kJ/mol (Figure S129), which is more favorable than the maximum $-\Delta H_{ads}$ measured for this material experimentally (55.9 ± 0.5 kJ/mol). In addition, the predicted ^{13}C NMR chemical shift for the HCO_3^- carbon is 166.0 ppm, significantly downfield from the observed resonance at 159.6 ppm (Figure 3). Because the IR spectra of all prepared CD-MOFs possess a shift at 1600 cm^{-1} due to permanently bound H_2O, even after activation (Figure 3a),[68] we hypothesize that permanently co-adsorbed H_2O might be playing a hitherto unrealized role in CO_2 chemisorption in CD-MOFs that accounts for these discrepancies. Indeed, the addition of a co-adsorbed water molecule to both the starting OH^- and final HCO_3^- sites in KOH CD-MOF (Figure 4) led to an improved match of the predicted $-\Delta E_{ads}$ (47.7 kJ/mol) and HCO_3^- ^{13}C NMR chemical shift (164.2 ppm) compared to the experimental values (Table 2). The discrepancy between the experimental and calculated ^{13}C NMR chemical shifts is in line with previous studies.[69] The reduction in favorable CO_2 binding in the presence of water is likely due to H_2O interacting more strongly with the OH^- sites in KOH CD-MOF than with the HCO_3^- sites in CO_2-dosed KOH CD-MOF. This is exhibited by the shorter predicted HO–H···OH^- distance (1.59 Å) in H_2O-bound KOH CD-MOF compared to the predicted HO–H···OCO_2H^- distance (2.16 Å) in H_2O-bound KOH CD-MOF after HCO_3^- formation (Figure 4). Moreover, DFT-calculated structures for the proposed binding modes of CO_2 in RbOH CD-MOF were determined, including via HCO_3^- formation (Figure 1e), via alkyl carbonate formation involving the primary alcohols of the D-glucopyranose units (Figure 1d), and via physisorption, and the computed CO_2 binding energies for each mechanism were compared in the absence and presence of water (Table 2, SI Figures S131–136). With or without permanently co-adsorbed water, CO_2 capture via bicarbonate formation was by far the preferred pathway in RbOH CD-MOF. Similar to KOH CD-MOF, the calculated $-\Delta E_{ads}$ for bicarbonate formation in the presence of water (53.5 kJ/mol) was similar to the experimental $-\Delta H_{ads}$ for this material (56 kJ/mol, see below). Together, these computational studies support that HCO_3^- formation at charge-balancing OH^- sites in the presence of strongly bound H_2O is the preferred pathway for CO_2 capture in CD-MOFs.

Cation effects on CO_2 capture. Given the close proximity between the OH^-/HCO_3^- species and the M^+ cations in DFT-calculated structures (Figure 4), we hypothesized that, if the proposed mechanism is operative, then changing the cation should also have a significant effect on CO_2 chemisorption in these materials (Figure 1e). In contrast, the cation would not be expected to significantly affect the strength of CO_2 binding via reaction at the D-glucopyranose R-OH units (Figures 1c–d). To probe this possibility, we prepared CD-MOFs bearing different cations for comparison with the K-based frameworks discussed above (see SI section 2 for details). Following the literature procedure, cubic RbOH CD-MOF was prepared via vapor diffusion.[54] Although attempts to prepare the isostructural framework NaOH CD-MOF via vapor diffusion were unsuccessful, in line with literature reports,[58] this material could be prepared under solvothermal conditions for the first time (SI Figure S36). As such, NaOH CD-MOF represents a rare example of a porous and crystalline Na-based MOF. Unfortunately, attempts to prepare isostructural frameworks from $NaHCO_3$ and Na_2CO_3 via vapor diffusion or under solvothermal conditions were unsuccessful. The preparation of CsOH CD-MOF under solvothermal conditions produced phase-pure CD-MOF-4 (SI Figure S29), in contrast with the challenges associated with producing phase-pure material using vapor diffusion (SI Figure S28).[58] Last, single-crystalline Cs_2CO_3 CD-MOF was prepared for the first time and could be structurally characterized by single-crystal X-ray diffraction (CCDC Structure Deposition #2161791, see SI Section 9 for details). Intriguingly, charge-balancing (bi)carbonates could be resolved within the pores of Cs_2CO_3 CD-MOF (SI Figure S144), consistent with the proposed mechanism for CO_2 capture in CD-MOFs (Figure 4). The promising results obtained herein for synthesizing K-, Na-, and Cs-based CD-MOFs under solvothermal conditions suggests that this avenue may be superior to vapor diffusion for preparing CD-MOFs that are otherwise challenging to access.

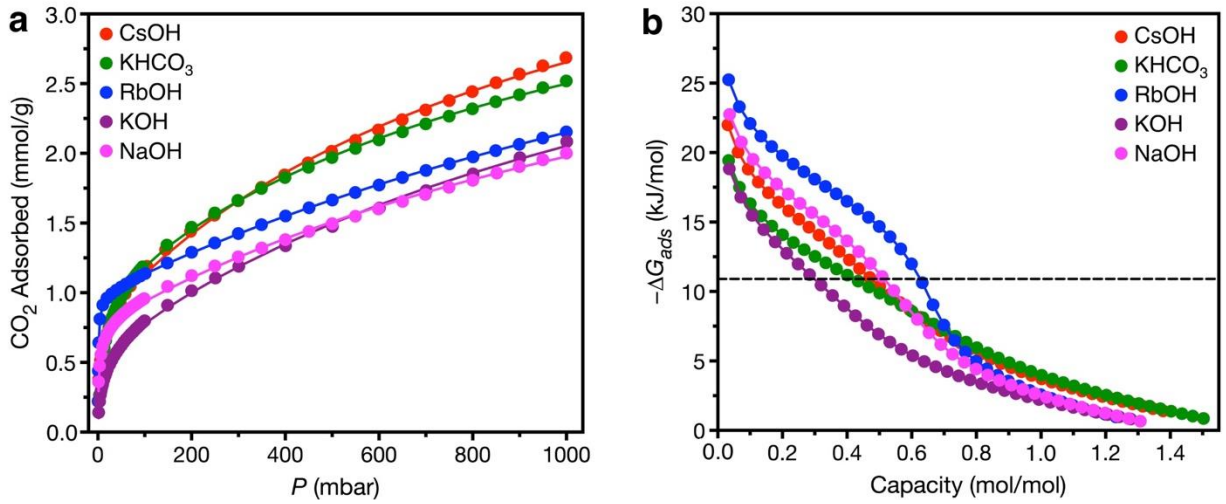

Figure 5. a) CO_2 adsorption isotherms of activated OH^--containing CD-MOFs with varying cations at 40 °C. $KHCO_3$ CD-MOF is included as a comparison. Solid lines represent fits to the dual-site Langmuir model. A data point was considered equilibrated when less than 0.01% change in pressure occurred over a 45 s interval. b) Free energies of adsorption ($-\Delta G_{ads}$) for CO_2 adsorption as a function of loading for CD-MOFs with varying cations. Materials that have $-\Delta G_{ads}$ values above the dashed line at 10.9 kJ/mol can adsorb CO_2 at a 90% capture rate from a coal flue gas stream, as determined using the equation $\Delta G = RT\ln(P/P_0)$ with T = 313 K, P = 15 mbar, and P_0 = 1 bar.[60]

Table 3. CO_2 uptakes and $-\Delta G_{ads}$ values at 40 °C for CD-MOFs with varying cations.

MOF	CO_2 uptake at 15 mbar (mmol/g)	CO_2 uptake at 1 bar (mmol/g)	$-\Delta G_{ads}$ at 40 °C (kJ/mol)
NaOH CD-MOF	0.70	1.98	22.7
RbOH CD-MOF	0.95	2.15	25.2
CsOH CD-MOF	0.67	2.65	22.0

As with K-based MOFs, CO_2 adsorption/desorption isotherms at 30 °C, 40 °C, and 50 °C and N_2 adsorption isotherms at 40 °C were measured for RbOH, NaOH, and CsOH CD-MOFs, and the CO_2 adsorption isotherms were fit using dual-site Langmuir models to yield $-\Delta H_{ads}$, $-\Delta S_{ads}$, and $-\Delta G_{ads}$ values (Figure 5, see SI section 3 for details). The CO_2 isotherms of Cs_2CO_3 CD-MOF showed poor CO_2 capacity, and therefore this material was not studied further (SI Figure S91). The 40 °C adsorption isotherms of RbOH, NaOH, and CsOH CD-MOFs in comparison to KOH CD-MOF and $KHCO_3$ CD-MOF (included for reference) reveal significant differences (Figure 5a), confirming that changing the cation modulates the CO_2 adsorption properties of CD-MOFs. At 1 bar of CO_2 and 40 °C, the observed trend in CO_2 capacities is CsOH CD-MOF (2.65 mmol/g) > RbOH CD-MOF (2.15 mmol/g) > KOH CD-MOF (2.06 mmol/g) > NaOH CD-MOF (1.98 mmol/g) (Table 3). This result may be due in part to the superior robustness of CD-MOFs prepared from larger alkali metal cations leading to higher accessible pore volumes.[58] Notably, this trend does not hold in the low pressure regime (SI Figure S95). At 15 mbar and 40 °C (representing >90% capture from a coal flue gas stream),[59] the observed capacity trend is RbOH CD-MOF (0.95 mmol/g) > NaOH CD-MOF (0.70 mmol/g) ≈ CsOH CD-MOF (0.67 mmol/g) > KOH CD-MOF (0.42 mmol/g); $KHCO_3$ CD-MOF displays similar uptake (0.63 mmol/g) as NaOH and CsOH CD-MOFs under these conditions. The observed trend in CO_2 uptake at low pressures is mirrored well in the $-\Delta G_{ads}$ values of these materials (Figure 5b and Table 3). In general, more thermodynamically favorable CO_2 capture is expected for metal hydroxide salts bearing heavier cations,[33] consistent with the strongest uptake occurring in RbOH CD-MOF. The unexpectedly weaker binding observed in CsOH CD-MOF may be due to the change in structure for this material (hexagonal) compared to the other MOH CD-MOFs (cubic). Overall, these results confirm that the cation making up CD-MOFs has a significant effect on their CO_2 capture properties, which is inconsistent with CO_2 capture at the D-glucopyranose units (Figures 1c–d).

Although significant differences were observed among MOH CD-MOFs (M = Na, K, Rb, Cs), gas sorption and spectroscopic studies suggest that they chemisorb CO_2 via a similar pathway. Indeed, the $-\Delta G_{ads}$ values for these materials at low loadings are all significantly higher in magnitude than those observed for frameworks lacking OH^- sites (Figure 2b and Table 3). In addition, the formation of a new carbonyl stretch upon exposure to CO_2 was observed in the TIR spectrum of NaOH CD-MOF (1668 cm^{-1}, SI Figure S108), which is consistent with the new carbonyl stretch observed in KOH CD-MOF (1663 cm^{-1}, Figure 3a) under the same conditions. Unfortunately, the presence of strongly bound water obscures this regime in CsOH and RbOH CD-MOFs (SI Figures S109 and S110). Last, as discussed above, DFT calculations support the feasibility of CO_2 capture via HCO_3^- formation in RbOH CD-MOF in the presence of water (SI Figure S132) by an analogous mechanism as predicted for KOH CD-MOF (Figure 4). The more favorable CO_2 binding in RbOH CD-MOF ($-\Delta E_{ads}$ = 53.5 kJ/mol) compared to KOH CD-MOF ($-\Delta E_{ads}$ = 47.7 kJ/mol) is reflected in the longer predicted $Rb^+\cdots OH^-$ distance (2.98 Å) than the $K^+\cdots OH^-$ (2.85 Å) distance and the shorter $Rb^+\cdots HCO_3^-$ (3.51 Å) distance than the $K^+\cdots HCO_3^-$ distance (3.55 Å) in the corresponding DFT-calculated structures. This shift indicates that soft HCO_3^- binds to the soft Rb^+ sites more strongly, favoring the adsorption product, whereas hard OH^- binds to the hard K^+ sites more strongly, disfavoring the adsorption product relative to the starting material. Since OH^- is bound less

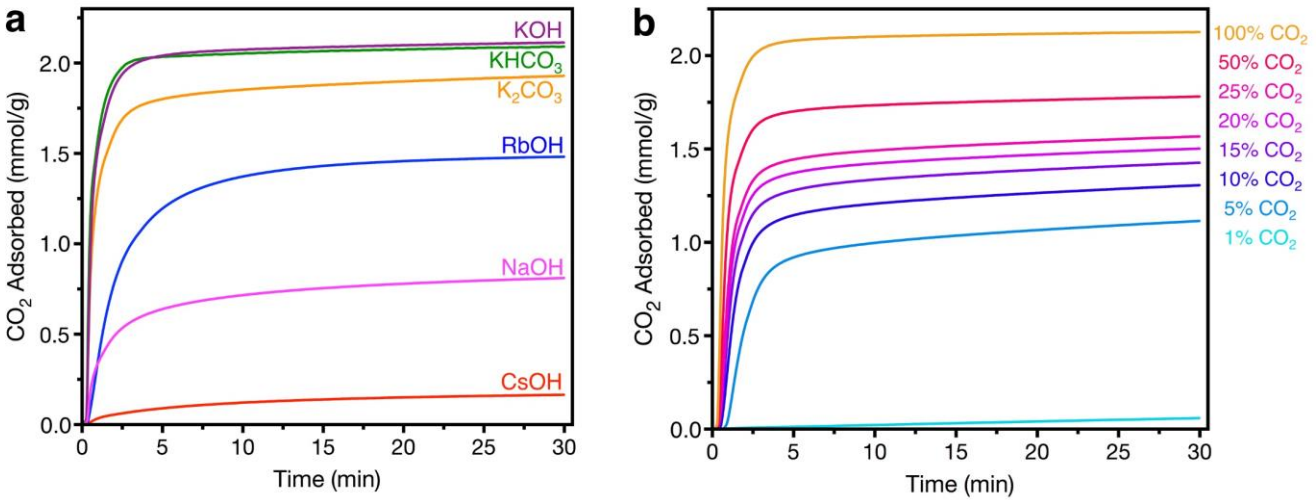

Figure 6. a) Pure CO_2 adsorption isotherms at 30 °C as measured by TGA for CD-MOFs after exposure to a flow of dry N_2 for 30 min at the optimal activation temperature for each CD-MOF (70 °C for KOH; 80 °C for $KHCO_3$; 110 °C for K_2CO_3; 120 °C for RbOH; 30 °C for NaOH; 30 °C for CsOH). b) Adsorption isotherms at different percentages of CO_2 in N_2 at 30 °C as measured by TGA for $KHCO_3$ CD-MOF. The sample was (re-)activated with dry N_2 at 80 °C for 30 min between measurements.

strongly and HCO_3^- is bound more strongly in RbOH CD-MOF, CO_2 capture via HCO_3^- formation is predicted to be more favorable in RbOH CD-MOF, in line with experimental findings (Figure 5). These findings support that M···OH^- interactions offers a handle to tune CO_2 capture affinities of CD-MOFs.[40,41]

CO_2 capture under realistic conditions. Having established the likely mechanism of CO_2 capture at OH^- sites in CD-MOFs, we next evaluated their potential for CO_2 capture from an idealized coal flue gas stream (15% CO_2 in N_2, 40 °C) as a representative separation. Owing to the chemisorptive pathway for CO_2 adsorption, all CD-MOFs bearing nucleophilic counteranions exhibit relatively high non-competitive CO_2/N_2 selectivities (S) under flue gas conditions in volumetric measurements (SI Table S14), including KOH (S = 61), $KHCO_3$ (S = 81), K_2CO_3 (S = 78), NaOH (S = 56), RbOH (S = 90), and CsOH (S = 126) CD-MOFs. Notably, these values are all higher than the non-competitive CO_2/N_2 selectivity of KOBz CD-MOF (S = 33). However, volumetric measurements are conducted under idealized conditions, such that activation is performed under high vacuum (<10 μbar) and pure gas is dosed in increments. Previous studies have shown that thermogravimetric analysis (TGA) measurements are better predictors of CO_2 capture performance under realistic conditions because they involve flowing gas mixtures over the sample instead.[42,70] In addition, TGA enables rapid evaluation of CO_2 adsorption kinetics under mixed gas conditions.[71] Hence, CO_2 adsorption in CD-MOFs bearing nucleophilic counteranions was next studied using TGA (Figures 6–7, see SI Section 5 for details).

The CO_2 capture performance of CD-MOFs was first evaluated by flowing pure CO_2 at atmospheric pressure over activated samples at 30 °C (Figure 6a). The optimal activation temperature of each CD-MOF under flowing N_2 was systematically determined using TGA to facilitate comparisons among optimally activated samples (see SI Section 5 for details). After 30 min, activated $KHCO_3$ and KOH CD-MOFs exhibited the highest CO_2 capacities (2.09 mmol/g and 2.11 mmol/g, respectively), followed by RbOH CD-MOF (1.48 mmol/g). In addition, $KHCO_3$ and KOH CD-MOFs nearly saturated in less than 2 min, demonstrating rapid CO_2 adsorption kinetics. Promisingly, $KHCO_3$ CD-MOF exhibited rapid CO_2 uptake from a 15% CO_2 in N_2 stream with a high capacity (1.43 mmol/g) as well (Figure 6b). In contrast, NaOH CD-MOF (0.81 mmol/g) and CsOH CD-MOF (0.16 mmol/g) exhibited low CO_2 uptakes by TGA, likely due to their poor thermal stabilities. Critically, when CO_2 adsorption was measured by TGA on a sample of KOH CD-MOF that had been soaked in dichloromethane for one week (the typical storage method of CD-MOFs), the MOF retained only 2% of its capacity, reflecting its modest long-term stability on the bench-top (SI Figure S123). In contrast, a sample of $KHCO_3$ CD-MOF that had been soaked in dichloromethane for two months retained 89% of its CO_2 capacity under the same conditions (SI Figure S122). This finding further supports the unexpectedly superior stability of $KHCO_3$ CD-MOF compared to KOH CD-MOF (SI Figures S103–104), confirming that the counteranion used during CD-MOF synthesis has a significant effect on the material's stability and CO_2 affinity. Due to its robustness, scalable synthesis, and rapid uptake of CO_2 under both volumetric and thermogravimetric conditions, $KHCO_3$ CD-MOF was selected as the most promising framework for further evaluation.

Beyond adsorption capacity, the long-term stability of an adsorbent is a critical consideration for industrial applications. In particular, the O_2 content of the coal flue gas stream is well known to lead to oxidative degradation of amine-based materials.[12,14,24] To evaluate the oxidative stability of $KHCO_3$ CD-MOF, the material was exposed to flowing dry air at 40 °C and atmospheric pressure for 12 h, and dry, pure CO_2 adsorption isobars were compared before and after exposure. Minimal changes were observed in the CO_2 adsorption profile after this extensive exposure to O_2, confirming the stability of $KHCO_3$ CD-MOF towards a much higher partial pressure of O_2 (~21%) than is present in flue emissions (4%) (Figure 7a). Minimal changes were also observed in the CO_2 adsorption profile of $KHCO_3$ CD-MOF after heating under flowing N_2 at 80 °C for 12 h (simulating numerous regeneration cycles), reflecting its promising thermal stability as well (Figure 7a).

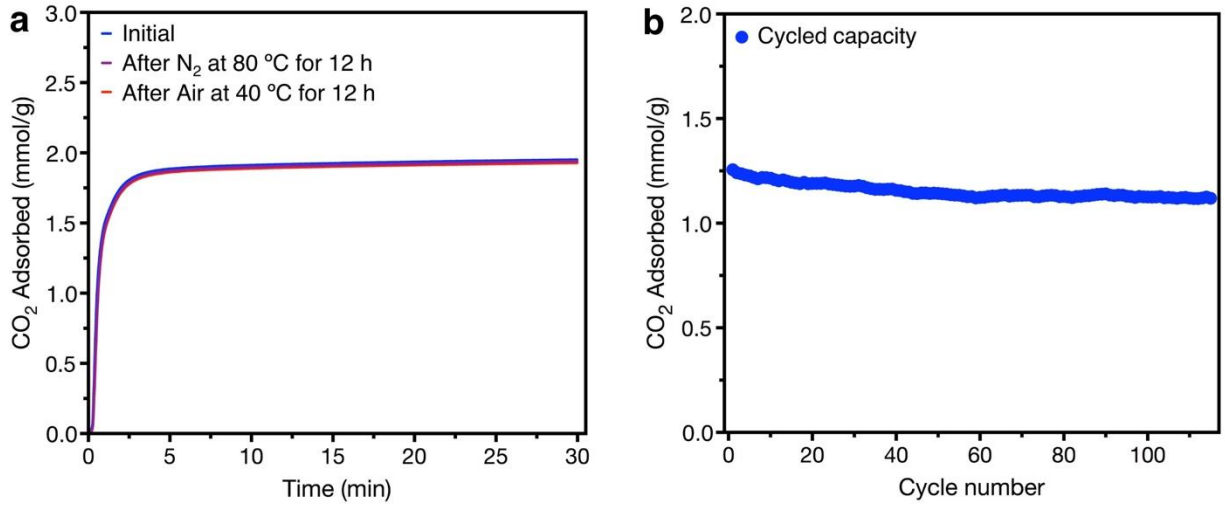

Figure 7. a) Dry, pure CO_2 adsorption isotherms for $KHCO_3$ CD-MOF after activation under flowing dry N_2 at 40 °C for 2 h and then at 80 °C for 1 h (blue curve), after exposure to flowing dry N_2 at 80 °C for 12 h (purple curve), and after exposure to flowing dry air (~21% O_2 in N_2) at 40 °C for 12 h (red curve). b) Cycling capacities for 115 adsorption/desorption cycles for $KHCO_3$ CD-MOF in a simulated temperature-pressure swing adsorption process. Adsorption: dry 15% CO_2 in N_2, 40 °C, 30 min. Desorption: dry, pure N_2, 80 °C, 30 min. The cycled capacity (difference) is shown.

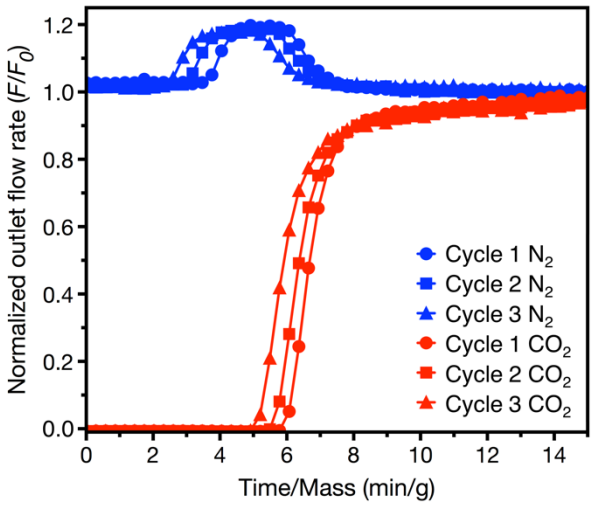

Figure 8. Breakthrough experiments with 0.520 g $KHCO_3$ CD-MOF under 25 sccm of a stream of dry 15% CO_2 in N_2 at 40 °C. CO_2 capacities: 1.22, 1.19, and 1.13 mmol/g for 1st, 2nd and 3rd cycles, respectively. N_2 capacities <0.1 mmol/g in all cases.

The thermal and oxidative stability of $KHCO_3$ CD-MOF encouraged us to evaluate its performance in a simulated temperature-pressure swing adsorption process using a N_2 purge as a stand-in for a pressure swing. As such, $KHCO_3$ CD-MOF was subjected to 115 adsorption (dry 15% CO_2 in N_2, 40 °C) and desorption (dry, pure N_2, 80 °C) cycles using TGA (Figure 7b, see SI Figure S125 for the full cycling data). Consistent with the accelerated decomposition test results (Figure 7a), $KHCO_3$ CD-MOF exhibited a stable cycling capacity (assuming negligible N_2 uptake), retaining approximately 90% of its CO_2 capacity after 115 cycles. A similar retention in capacity (91%) was observed after 100 cycles with an adsorption temperature of 30 °C on an independently prepared sample of $KHCO_3$ CD-MOF (SI Figure S126).

To evaluate the performance of $KHCO_3$ CD-MOF in a fixed-bed adsorption process, we conducted breakthrough experiments with dry simulated coal flue gas using a custom-built apparatus (see SI section 8 for details). Breakthrough experiments were carried out by subjecting 0.520 g of activated $KHCO_3$ CD-MOF to 25 sccm of dry 15% CO_2 in N_2 at 40 °C (Figure 8). Under these conditions, N_2 broke through the column nearly instantly, followed much later by CO_2. Importantly, the CO_2 breakthrough profile was sharp, reflecting the fast adsorption kinetics in this material. The breakthrough CO_2 capacity was calculated to be 1.18 ± 0.05 mmol/g (average of three experiments), which is comparable to the CO_2 capacity of 1.26 mmol/g measured under a stream of 15% CO_2 in N_2 by TGA (Figure 7b). Consistent with the 40 °C N_2 adsorption isotherm of this material (SI Figure S97), its N_2 capacity was found to be negligible (<0.1 mmol/g). Critically, the breakthrough profile and capacity of $KHCO_3$ CD-MOF were reproducible over three cycles following re-activation of the material at 40 °C under flowing He (Figure 8). A breakthrough experiment under humid conditions was also conducted using 25 sccm of humidified 15% CO_2 in N_2 at 40 °C after the MOF was pre-humidified using humid He (approximately 23% relative humidity at 20 °C, SI Figure S142). Though the CO_2 adsorption capacity of the material under humid conditions (0.43 mmol/g) was lower than that under dry conditions (1.13 mmol/g, cycle 3), selective CO_2 binding over N_2 was still observed (SI Figure S142). Importantly, $KHCO_3$ CD-MOF retained its crystallinity after the humid breakthrough experiment, confirming its stability towards humidified gas streams (SI Figure S143). As such, the reduction in CO_2 capacity under humidified conditions is likely due to filling of the hydrophilic pores with H_2O, blocking access of CO_2 to reactive OH^- sites,[42] and not due to degradation of $KHCO_3$ CD-MOF under these conditions. Overall, due to its thermal robustness, oxidative stability, and good performance in cycling and breakthrough experiments, $KHCO_3$ CD-MOF is a promising new material for further study of CO_2 capture from coal flue gas emissions, though further optimization is required to improve its CO_2 capacity under humid conditions.

CONCLUSION

Through extensive gas sorption, spectroscopic, and computational studies, we have demonstrated that reversible CO_2 capture is feasible at charge-balancing OH^- sites within the pores of CD-MOFs (Figure 1e). Our findings advance the understanding of the carbon capture pathway in these materials and suggest that the previously proposed carbonic acid and alkyl carbonate pathways are likely not operative (Figure 1c–d). The observed requirement for nucleophilic counteranions in the pores rules out carbonic acid formation (Figure 1c), whereas the observed cation effect, reversibility of CO_2 adsorption upon cycling, ^{13}C SSNMR chemical shift, and DFT calculations are inconsistent with alkyl carbonate formation (Figure 1d). Careful evaluation of the effect of the framework cation and anion revealed that inexpensive $KHCO_3$ CD-MOF is the most promising framework for CO_2 capture under realistic, mixed gas conditions. In contrast to the isostructural KOH CD-MOF, this material retains its structural integrity after accelerated decomposition tests, under oxidizing conditions, and after exposure to humidity. Moreover, the cation of CD-MOFs represents a potential tuning handle for adjusting their CO_2 adsorption thermodynamics, as Rb-based CD-MOFs display generally stronger CO_2 binding affinity (albeit with lower capacities) than K-based CD-MOFs. Our computational results suggest this is due to differing interactions between OH^-/HCO_3^- sites and the cations within these two materials. Additionally, our experimental and computational findings highlight a potential hitherto unrecognized role for permanently adsorbed water in CD-MOFs on CO_2 capture within these materials.[68]

It is worth noting that, unlike OH^--containing CD-MOFs, the corresponding bulk MOH salts generally display poor reactivity towards dry CO_2 in the solid state.[35,36] As such, our results suggest that disrupting the M–OH lattice is sufficient to promote the nucleophilicity of OH^- sites towards CO_2 under mild conditions. As such, the incorporation of OH^- sites within porous frameworks represents a potentially general strategy for the design of new, oxidation-resistant adsorbents for carbon capture that are potentially competitive with amine-based technologies. Future work will focus on the synthesis of new CD-MOFs with less hydrophilic pore environments with improved CO_2 capacities under humid conditions.

ASSOCIATED CONTENT

Supporting Information. Characterization data and details of all experiments. This material is available free of charge via the Internet at http://pubs.acs.org. The single-crystal X-ray diffraction structure of Cs_2CO_3 CD-MOF is available via the Cambridge Crystallographic Data Centre (CCDC Deposition #2161791).

AUTHOR INFORMATION

Corresponding Author

* pjm347@cornell.edu

Author Contributions

P.J.M. and A.C.F. conceived the project. M.E.Z. prepared and characterized all samples and carried out all IR, gas adsorption, and breakthrough measurements. S.M.P. carried out all SSNMR experiments. J.H.L. carried out all DFT calculations. The manuscript was written through the contributions of all authors and all authors approved of the final version.

Funding Sources

This work was supported by the U.S. Department of Energy, Office of Science, Office of Basic Energy Sciences under Award Number DE-SC0021000 (M.E.Z., P.J.M.). The collection of single-crystal X-ray diffraction data was partially supported by the Cornell Center for Materials Research with funding from the National Science Foundation MRSEC program (DMR-1719875). This work is based upon research conducted at the Northeastern Collaborative Access Team beamlines, which are funded by the National Institute of General Medical Sciences from the National Institutes of Health (P30 GM124165). This research used resources of the Advanced Photon Source, a U.S. Department of Energy (DOE) Office of Science User Facility operated for the DOE Office of Science by Argonne National Laboratory under Contract No. DE-AC02-06CH11357. A.C.F. and S.M.P. were supported by a UKRI Future Leaders Fellowship to A.C.F. (MR/T043024/1), and a Leverhulme Trust Research Project Grant (RPG-2020-337) to A.C.F. A.C.F. also thanks the Yusuf Hamied Department of Chemistry (Cambridge) for the award of a BP Next Generation Fellowship. J.H.L. was supported by the KIST Institutional Program (Project No. 2E31201) with computational resources provided by the KISTI Supercomputing Center (Project No. KSC-2020-CRE-0189). J.H.L.'s work was further supported by the program of Future Hydrogen Original Technology Development (2021M3I3A1083946), through the National Research Foundation of Korea (NRF), funded by the Korean government (Ministry of Science and ICT (MSIT)). Some of the solution-state NMR spectra in this work were collected on a Bruker INOVA 500 MHZ spectrometer that was purchased with support from the National Science Foundation (CHE-1531632).

Notes

P.J.M. is listed as a co-inventor on several patents related to MOFs.

ACKNOWLEDGMENT

We thank Samantha MacMillan (Cornell University) for solving the single-crystal X-ray diffraction structure of Cs_2CO_3 CD-MOF and Tristan Pitt (Cornell University) for collecting SEM and EDX data for KCl CD-MOF. We thank Dr. Rebecca Siegelman (DuPont) for assistance with breakthrough measurements and Michael Patterson and Prof. Nozomi Ando (Cornell University) for assistance with preparing samples for single-crystal X-ray diffraction. We are grateful to Ruth Mandel and Jaehwan Kim (Cornell University) for editorial assistance during the preparation of this manuscript.

REFERENCES

(1) Climate Change 2021: The Physical Science Basis. Contribution of Working Group I to the Sixth Assessment Report of the Intergovernmental Panel on Climate Change; Masson-Delmotte, V., Zhai, P., Pirani, A., Connors, S. L., Péan, C., Berger, S., Caud, N., Chen, Y., Goldfarb, L., Gomis, M. I., Huang, M., Leitzell, K., Lonnoy, E., Matthews, J. B. R., Maycock, T. K., Waterfield, T., Yelekçi, Ö., Yu, R., Zhou, B., Eds.; Cambridge University Press, 2021.

(2) CO_2 Emissions from Fuel Combustion: Overview; International Energy Agency: Paris, France, 2017.

(3) Chu, S. Carbon Capture and Sequestration. *Science* **2009**, 325 (5948), 1599–1599. https://doi.org/10.1126/science.1181637.

(4) Siegelman, R. L.; Kim, E. J.; Long, J. R. Porous Materials for Carbon Dioxide Separations. *Nat. Mater.* **2021**, 20 (8), 1060–1072. https://doi.org/10.1038/s41563-021-01054-8.

(5) Siegelman, R. L.; Milner, P. J.; Kim, E. J.; Weston, S. C.; Long, J. R. Challenges and Opportunities for Adsorption-Based CO_2 Capture from Natural Gas Combined Cycle Emissions. *Energy Environ. Sci.* **2019**, 12 (7), 2161–2173. https://doi.org/10.1039/C9EE00505F.

(6) Bui, M.; Adjiman, C. S.; Bardow, A.; Anthony, E. J.; Boston, A.; Brown, S.; Fennell, P. S.; Fuss, S.; Galindo, A.; Hackett, L. A.; Hallett, J. P.; Herzog, H. J.; Jackson, G.; Kemper, J.; Krevor, S.; Maitland, G. C.; Matuszewski, M.; Metcalfe, I. S.; Petit, C.; Puxty, G.; Reimer, J.; Reiner, D. M.; Rubin, E. S.; Scott, S. A.; Shah, N.; Smit, B.; Trusler, J. P. M.; Webley, P.; Wilcox, J.; Mac Dowell, N. Carbon Capture and Storage (CCS): The Way Forward. *Energy Environ. Sci.* 2018, *11*, 1062–1176. https://doi.org/10.1039/C7EE02342A.

(7) Barker, D. J.; Turner, S. A.; Napier-Moore, P. A.; Clark, M.; Davison, J. E. CO_2 Capture in the Cement Industry. *Energy Procedia* **2009**, 1 (1), 87–94. https://doi.org/10.1016/j.egypro.2009.01.014.

(8) Sanz-Pérez, E. S.; Murdock, C. R.; Didas, S. A.; Jones, C. W. Direct Capture of CO_2 from Ambient Air. *Chem. Rev.* **2016**, 116 (19), 11840–11876. https://doi.org/10.1021/acs.chemrev.6b00173.

(9) McQueen, N.; Gomes, K. V.; McCormick, C.; Blumanthal, K.; Pisciotta, M.; Wilcox, J. A Review of Direct Air Capture (DAC): Scaling up Commercial Technologies and Innovating for the Future. *Prog. Energy* **2021**, 3 (3), 032001. https://doi.org/10.1088/2516-1083/abf1ce.

(10) Direct Air Capture – Analysis https://www.iea.org/reports/direct-air-capture (accessed 2022 -01 -18).

(11) Gary T. Rochelle. Amine Scrubbing for CO_2 Capture. *Science* **2009**, 325 (5948), 1647–1652. https://doi.org/10.1126/science.1172246.

(12) Vega, F.; Sanna, A.; Navarrete, B.; Maroto-Valer, M. M.; Cortés, V. J. Degradation of Amine-Based Solvents in CO_2 Capture Process by Chemical Absorption. *Greenhouse Gas Sci. Technol.* **2014**, 4 (6), 707–733. https://doi.org/10.1002/ghg.1446.

(13) Fredriksen, S. B.; Jens, K.-J. Oxidative Degradation of Aqueous Amine Solutions of MEA, AMP, MDEA, Pz: A Review. *Energy Procedia* **2013**, 37, 1770–1777. https://doi.org/10.1016/j.egypro.2013.06.053.

(14) Gouedard, C.; Picq, D.; Launay, F.; Carrette, P.-L. Amine Degradation in CO_2 Capture. I. A Review. *Int. J. Greenh. Gas Control* **2012**, 10, 244–270. https://doi.org/10.1016/j.ijggc.2012.06.015.

(15) Chi, S.; Rochelle, G. T. Oxidative Degradation of Monoethanolamine. *Ind. Eng. Chem. Res.* **2002**, 41 (17), 4178–4186. https://doi.org/10.1021/ie010697c.

(16) Heldebrant, D. J.; Koech, P. K.; Glezakou, V.-A.; Rousseau, R.; Malhotra, D.; Cantu, D. C. Water-Lean Solvents for Post-Combustion CO_2 Capture: Fundamentals, Uncertainties, Opportunities, and Outlook. *Chem. Rev.* **2017**, 117 (14), 9594–9624. https://doi.org/10.1021/acs.chemrev.6b00768.

(17) Dutcher, B.; Fan, M.; Russell, A. G. Amine-Based CO_2 Capture Technology Development from the Beginning of 2013—A Review. *ACS Appl. Mater. Interfaces* **2015**, 7 (4), 2137–2148. https://doi.org/10.1021/am507465f.

(18) Kim, C.; Cho, H. S.; Chang, S.; Cho, S. J.; Choi, M. An Ethylenediamine-Grafted Y Zeolite: A Highly Regenerable Carbon Dioxide Adsorbent via Temperature Swing Adsorption without Urea Formation. *Energy Environ. Sci.* **2016**, 9 (5), 1803–1811. https://doi.org/10.1039/C6EE00601A.

(19) Bollini, P.; Didas, S. A.; Jones, C. W. Amine-Oxide Hybrid Materials for Acid Gas Separations. *J. Mat. Chem.* **2011**, 21 (39), 15100. https://doi.org/10.1039/c1jm12522b.

(20) Ding, M.; Flaig, R. W.; Jiang, H.-L.; Yaghi, O. M. Carbon Capture and Conversion Using Metal–Organic Frameworks and MOF-Based Materials. *Chem. Soc. Rev.* **2019**, 48 (10), 2783–2828. https://doi.org/10.1039/C8CS00829A.

(21) Trickett, C. A.; Helal, A.; Al-Maythalony, B. A.; Yamani, Z. H.; Cordova, K. E.; Yaghi, O. M. The Chemistry of Metal–Organic Frameworks for CO_2 Capture, Regeneration and Conversion. *Nat. Rev. Mat.* **2017**, 2 (8), 17045. https://doi.org/10.1038/natrevmats.2017.45.

(22) Lin, Y.; Kong, C.; Chen, L. Amine-Functionalized Metal–Organic Frameworks: Structure, Synthesis and Applications. *RSC Adv.* **2016**, 6 (39), 32598–32614. https://doi.org/10.1039/C6RA01536K.

(23) Yoo, C.-J.; Park, S. J.; Jones, C. W. CO_2 Adsorption and Oxidative Degradation of Silica-Supported Branched and Linear Aminosilanes. *Ind. Eng. Chem. Res.* **2020**, 59 (15), 7061–7071. https://doi.org/10.1021/acs.iecr.9b04205.

(24) Mazari, S. A.; Si Ali, B.; Jan, B. M.; Saeed, I. M.; Nizamuddin, S. An Overview of Solvent Management and Emissions of Amine-Based CO_2 Capture Technology. *Int. J. Greenh. Gas Control* **2015**, 34, 129–140. https://doi.org/10.1016/j.ijggc.2014.12.017.

(25) Ahmadalinezhad, A.; Sayari, A. Oxidative Degradation of Silica-Supported Polyethylenimine for CO_2 Adsorption: Insights into the Nature of Deactivated Species. *Phys. Chem. Chem. Phys.* **2014**, 16 (4), 1529–1535. https://doi.org/10.1039/C3CP53928H.

(26) Bali, S.; Chen, T. T.; Chaikittisilp, W.; Jones, C. W. Oxidative Stability of Amino Polymer–Alumina Hybrid Adsorbents for Carbon Dioxide Capture. *Energy Fuels* **2013**, 27 (3), 1547–1554. https://doi.org/10.1021/ef4001067.

(27) Srikanth, C. S.; Chuang, S. S. C. Spectroscopic Investigation into Oxidative Degradation of Silica-Supported Amine Sorbents for CO_2 Capture. *ChemSusChem* **2012**, 5 (8), 1435–1442. https://doi.org/10.1002/cssc.201100662.

(28) Heydari-Gorji, A.; Sayari, A. Thermal, Oxidative, and CO_2-Induced Degradation of Supported Polyethylenimine Adsorbents. *Ind. Eng. Chem. Res.* **2012**, 51 (19), 6887–6894. https://doi.org/10.1021/ie3003446.

(29) Bollini, P.; Choi, S. Oxidative Degradation of Aminosilica Adsorbents Relevant to Postcombustion CO_2 Capture. *Energy Fuels* **2011**, 25 (5), 2416–2425.

(30) Heydari-Gorji, A.; Belmabkhout, Y.; Sayari, A. Degradation of Amine-Supported CO_2 Adsorbents in the Presence of Oxygen-Containing Gases. *Microporous Mesoporous Mater.* **2011**, 145 (1–3), 146–149. https://doi.org/10.1016/j.micromeso.2011.05.010.

(31) Liu, Y.; Ye, H.-Z.; Diederichsen, K. M.; Van Voorhis, T.; Hatton, T. A. Electrochemically Mediated Carbon Dioxide Separation with Quinone Chemistry in Salt-Concentrated Aqueous Media. *Nat. Commun.* **2020**, 11 (1), 2278. https://doi.org/10.1038/s41467-020-16150-7.

(32) Forse, A. C.; Milner, P. J. New Chemistry for Enhanced Carbon Capture: Beyond Ammonium Carbamates. *Chem. Sci.* **2021**, 12 (2), 508–516. https://doi.org/10.1039/D0SC06059C.

(33) Duan, Y.; Sorescu, D. C. CO_2 Capture Properties of Alkaline Earth Metal Oxides and Hydroxides: A Combined Density Functional Theory and Lattice Phonon Dynamics Study. *J. Chem. Phys.* **2010**, 133 (7), 074508. https://doi.org/10.1063/1.3473043.

(34) Mahmoudkhani, M.; Keith, D. W. Low-Energy Sodium Hydroxide Recovery for CO_2 Capture from Atmospheric Air—Thermodynamic Analysis. *Int. J. Greenh. Gas Control* **2009**, 3 (4), 376–384. https://doi.org/10.1016/j.ijggc.2009.02.003.

(35) Samari, M.; Ridha, F.; Manovic, V.; Macchi, A.; Anthony, E. J. Direct Capture of Carbon Dioxide from Air via Lime-Based Sorbents. *Mitig. Adapt. Strateg. Glob. Change* **2020**, 25 (1), 25–41. https://doi.org/10.1007/s11027-019-9845-0.

(36) Beruto, D. T.; Botter, R. Liquid-like H_2O Adsorption Layers to Catalyze the $Ca(OH)_2/CO_2$ Solid–Gas Reaction and to Form a Non-Protective Solid Product Layer at 20°C. *J. Eur. Ceram. Soc.* **2000**, 20 (4), 497–503. https://doi.org/10.1016/S0955-2219(99)00185-5.

(37) Pham, A. L.-T.; Sedlak, D. L.; Doyle, F. M. Dissolution of Mesoporous Silica Supports in Aqueous Solutions: Implications for Mesoporous Silica-Based Water Treatment Processes. *Appl. Catal. B* **2012**, 126, 258–264. https://doi.org/10.1016/j.apcatb.2012.07.018.

(38) Wang, Z.; Bilegsaikhan, A.; Jerozal, R. T.; Pitt, T. A.; Milner, P. J. Evaluating the Robustness of Metal–Organic Frameworks for Synthetic Chemistry. *ACS Appl. Mater. Interfaces* **2021**, 13 (15), 17517–17531. https://doi.org/10.1021/acsami.1c01329.

(39) Yuan, S.; Feng, L.; Wang, K.; Pang, J.; Bosch, M.; Lollar, C.; Sun, Y.; Qin, J.; Yang, X.; Zhang, P.; Wang, Q.; Zou, L.; Zhang, Y.; Zhang, L.; Fang, Y.; Li, J.; Zhou, H.-C. Stable Metal-Organic Frameworks: Design, Synthesis, and Applications. *Adv. Mater.* **2018**, 1704303. https://doi.org/10.1002/adma.201704303.

(40) Bien, C. E.; Liu, Q.; Wade, C. R. Assessing the Role of Metal Identity on CO_2 Adsorption in MOFs Containing M–OH Functional Groups. *Chem. Mater.* **2020**, 32 (1), 489–497. https://doi.org/10.1021/acs.chemmater.9b04228.

(41) Cai, Z.; Bien, C. E.; Liu, Q.; Wade, C. R. Insights into CO_2 Adsorption in M–OH Functionalized MOFs. *Chem. Mater.* **2020**, 32 (10), 4257–4264. https://doi.org/10.1021/acs.chemmater.0c00746.

(42) Bien, C. E.; Chen, K. K.; Chien, S.-C.; Reiner, B. R.; Lin, L.-C.; Wade, C. R.; Ho, W. S. W. Bioinspired Metal–Organic Framework for Trace CO_2 Capture. *J. Am. Chem. Soc.* **2018**, 140 (40), 12662–12666. https://doi.org/10.1021/jacs.8b06109.

(43) Wright, A. M.; Wu, Z.; Zhang, G.; Mancuso, J. L.; Comito, R. J.; Day, R. W.; Hendon, C. H.; Miller, J. T.; Dincă, M. A Structural Mimic of Carbonic Anhydrase in a Metal-Organic Framework. *Chem* **2018**, 4 (12), 2894–2901. https://doi.org/10.1016/j.chempr.2018.09.011.

(44) Liao, P.-Q.; Chen, H.; Zhou, D.-D.; Liu, S.-Y.; He, C.-T.; Rui, Z.; Ji, H.; Zhang, J.-P.; Chen, X.-M. Monodentate Hydroxide as a Super Strong yet Reversible Active Site for CO_2 Capture from High-Humidity Flue Gas. *Energy Environ. Sci.* **2015**, 8 (3), 1011–1016. https://doi.org/10.1039/C4EE02717E.

(45) Wang, T.; Lackner, K. S.; Wright, A. Moisture Swing Sorbent for Carbon Dioxide Capture from Ambient Air. *Environ. Sci. Technol.* **2011**, 45 (15), 6670–6675. https://doi.org/10.1021/es201180v.

(46) Xu, L.; Xing, C.-Y.; Ke, D.; Chen, L.; Qiu, Z.-J.; Zeng, S.-L.; Li, B.-J.; Zhang, S. Amino-Functionalized β-Cyclodextrin to Construct Green Metal–Organic Framework Materials for CO_2 Capture. *ACS Appl. Mater. Interfaces* **2020**, 12 (2), 3032–3041. https://doi.org/10.1021/acsami.9b20003.

(47) He, Y.; Hou, X.; Liu, Y.; Feng, N. Recent Progress in the Synthesis, Structural Diversity and Emerging Applications of Cyclodextrin-Based Metal–Organic Frameworks. *J. Mater. Chem. B* **2019**, 7 (37), 5602–5619. https://doi.org/10.1039/C9TB01548E.

(48) Li, L.; Wang, J.; Zhang, Z.; Yang, Q.; Yang, Y.; Su, B.; Bao, Z.; Ren, Q. Inverse Adsorption Separation of CO_2/C_2H_2 Mixture in Cyclodextrin-Based Metal–Organic Frameworks. *ACS Appl. Mater. Interfaces* **2019**, 11 (2), 2543–2550. https://doi.org/10.1021/acsami.8b19590.

(49) Patel, H. A.; Islamoglu, T.; Liu, Z.; Nalluri, S. K. M.; Samanta, A.; Anamimoghadam, O.; Malliakas, C. D.; Farha, O. K.; Stoddart, J. F. Noninvasive Substitution of K^+ Sites in Cyclodextrin Metal–Organic Frameworks by Li^+ Ions. *J. Am. Chem. Soc.* **2017**, 139 (32), 11020–11023. https://doi.org/10.1021/jacs.7b06287.

(50) Yan, T. K.; Nagai, A.; Michida, W.; Kusakabe, K.; Yusup, S. binti. Crystal Growth of Cyclodextrin-Based Metal-Organic Framework for Carbon Dioxide Capture and Separation. *Procedia Eng.* **2016**, 148, 30–34. https://doi.org/10.1016/j.proeng.2016.06.480.

(51) Gassensmith, J. J.; Kim, J. Y.; Holcroft, J. M.; Farha, O. K.; Stoddart, J. F.; Hupp, J. T.; Jeong, N. C. A Metal–Organic Framework-Based Material for Electrochemical Sensing of Carbon Dioxide. *J. Am. Chem. Soc.* **2014**, 136 (23), 8277–8282. https://doi.org/10.1021/ja5006465.

(52) Wu, D.; Gassensmith, J. J.; Gouvêa, D.; Ushakov, S.; Stoddart, J. F.; Navrotsky, A. Direct Calorimetric Measurement of Enthalpy of Adsorption of Carbon Dioxide on CD-MOF-2, a Green Metal–Organic Framework. *J. Am. Chem. Soc.* **2013**, 135 (18), 6790–6793. https://doi.org/10.1021/ja402315d.

(53) Gassensmith, J. J.; Furukawa, H.; Smaldone, R. A.; Forgan, R. S.; Botros, Y. Y.; Yaghi, O. M.; Stoddart, J. F. Strong and Reversible Binding of Carbon Dioxide in a Green Metal–Organic Framework. *J. Am. Chem. Soc.* **2011**, 133 (39), 15312–15315. https://doi.org/10.1021/ja206525x.

(54) Smaldone, R. A.; Forgan, R. S.; Furukawa, H.; Gassensmith, J. J.; Slawin, A. M. Z.; Yaghi, O. M.; Stoddart, J. F. Metal-Organic Frameworks from Edible Natural Products. *Angew. Chem. Int. Ed.* **2010**, 49 (46), 8630–8634. https://doi.org/10.1002/anie.201002343.

(55) Pham, H. D. M.; Khaliullin, R. Z. Unraveling the Origins of Strong and Reversible Chemisorption of Carbon Dioxide in a Green Metal–Organic Framework. *J. Phys. Chem. C* **2021**, 125 (44), 24719–24727. https://doi.org/10.1021/acs.jpcc.1c07610.

(56) Wang, C.; Luo, H.; Jiang, D.; Li, H.; Dai, S. Carbon Dioxide Capture by Superbase-Derived Protic Ionic Liquids. *Angew. Chem. Int. Ed.* **2010**, 49 (34), 5978–5981. https://doi.org/10.1002/anie.201002641.

(57) Drage, T. C.; Arenillas, A.; Smith, K. M.; Snape, C. E. Thermal Stability of Polyethylenimine Based Carbon Dioxide Adsorbents and Its Influence on Selection of Regeneration Strategies. *Microporous Mesoporous Mater.* **2008**, 116 (1–3), 504–512. https://doi.org/10.1016/j.micromeso.2008.05.009.

(58) Forgan, R. S.; Smaldone, R. A.; Gassensmith, J. J.; Furukawa, H.; Cordes, D. B.; Li, Q.; Wilmer, C. E.; Botros, Y. Y.; Snurr, R. Q.; Slawin, A. M. Z.; Stoddart, J. F. Nanoporous Carbohydrate Metal–Organic Frameworks. *J. Am. Chem. Soc.* **2012**, 134 (1), 406–417. https://doi.org/10.1021/ja208224f.

(59) Granite, E. J.; Pennline, H. W. Photochemical Removal of Mercury from Flue Gas. *Ind. Eng. Chem. Res.* **2002**, 41 (22), 5470–5476. https://doi.org/10.1021/ie020251b.

(60) Milner, P. J.; Siegelman, R. L.; Forse, A. C.; Gonzalez, M. I.; Runčevski, T.; Martell, J. D.; Reimer, J. A.; Long, J. R. A Diaminopropane-Appended Metal-Organic Framework Enabling Efficient CO_2 Capture from Coal Flue Gas via a Mixed Adsorption Mechanism. *J. Am. Chem. Soc.* **2017**, 139 (38), 13541–13553. https://doi.org/10.1021/jacs.7b07612.

(61) Krug, R. R.; Hunter, W. G.; Grieger, R. A. Statistical Interpretation of Enthalpy–Entropy Compensation. *Nature* **1976**, 261 (5561), 566–567. https://doi.org/10.1038/261566a0.

(62) International Symposium on Cyclodextrins, T. L., J. J.; Vila-Jato, J. L. Proceedings of the Ninth International Symposium on Cyclodextrins: Santiago de Compostela, Spain, May 31-June 3, 1998; Springer: Dordrecht, 1999.

(63) Looney, A.; Han, R.; McNeill, K.; Parkin, G. Tris(Pyrazolyl)Hydroboratozinc Hydroxide Complexes as Functional Models for Carbonic Anhydrase: On the Nature of the Bicarbonate Intermediate. *J. Am. Chem. Soc.* **1993**, 115 (11), 4690–4697. https://doi.org/10.1021/ja00064a033.

(64) Chen, C.-H.; Shimon, D.; Lee, J. J.; Mentink-Vigier, F.; Hung, I.; Sievers, C.; Jones, C. W.; Hayes, S. E. The "Missing" Bicarbonate in CO_2 Chemisorption Reactions on Solid Amine Sorbents. *J. Am. Chem. Soc.* **2018**, 140 (28), 8648–8651. https://doi.org/10.1021/jacs.8b04520.

(65) Sattler, W.; Parkin, G. Structural Characterization of Zinc Bicarbonate Compounds Relevant to the Mechanism of Action of Carbonic Anhydrase. *Chem. Sci.* **2012**, 3 (6), 2015. https://doi.org/10.1039/c2sc20167d.

(66) Kortunov, P. V.; Siskin, M.; Baugh, L. S.; Calabro, D. C. In Situ Nuclear Magnetic Resonance Mechanistic Studies of Carbon Dioxide Reactions with Liquid Amines in Aqueous Systems: New Insights on Carbon Capture Reaction Pathways. *Energy Fuels* **2015**, 29 (9), 5919–5939. https://doi.org/10.1021/acs.energyfuels.5b00850.

(67) Mani, F.; Peruzzini, M.; Stoppioni, P. CO_2 Absorption by Aqueous NH_3 Solutions: Speciation of Ammonium Carbamate, Bicarbonate and Carbonate by a ^{13}C NMR Study. *Green Chem.* **2006**, 8 (11), 995. https://doi.org/10.1039/b602051h.

(68) Kohata, S; Jyodoi, K.; Ohyoshi, A. Thermal Decomposition of Cyclodextrins (α-, β-, γ-, and Modified β-CyD) and of Metal-(β-CyD) Complexes in the Solid Phase. *Thermochim. Acta* **1993**, 217, 187–198. https://doi.org/10.1016/0040-6031(93)85107-K.

(69) Forse, A. C.; Milner, P. J.; Lee, J.-H.; Redfearn, H. N.; Oktawiec, J.; Siegelman, R. L.; Martell, J. D.; Dinakar, B.; Porter-Zasada, L. B.; Gonzalez, M. I.; Neaton, J. B.; Long, J. R.; Reimer, J. A. Elucidating CO_2 Chemisorption in Diamine-Appended Metal–Organic Frameworks. *J. Am. Chem. Soc.* **2018**, 140 (51), 18016–18031. https://doi.org/10.1021/jacs.8b10203.

(70) Liao, P.-Q.; Chen, X.-W.; Liu, S.-Y.; Li, X.-Y.; Xu, Y.-T.; Tang, M.; Rui, Z.; Ji, H.; Zhang, J.-P.; Chen, X.-M. Putting an Ultrahigh Concentration of Amine Groups into a Metal–Organic Framework for CO_2 Capture at Low Pressures. *Chem. Sci.* **2016**, 7 (10), 6528–6533. https://doi.org/10.1039/C6SC00836D.

(71) Martell, J. D.; Milner, P. J.; Siegelman, R. L.; Long, J. R. Kinetics of Cooperative CO_2 Adsorption in Diamine-Appended Variants of the Metal–Organic Framework Mg_2(dobpdc). *Chem. Sci.* **2020**, 11, 6457–6471. https://doi.org/10.1039/D0SC01087A.

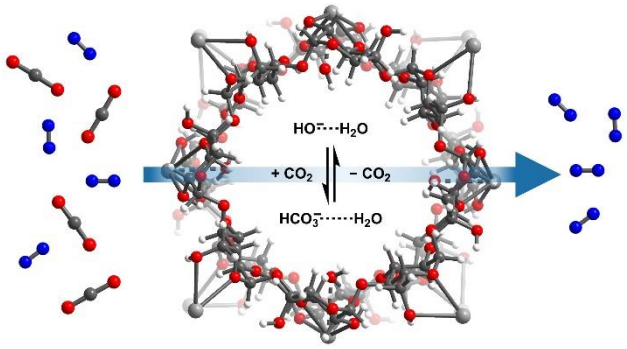
HO⁻···H₂O
+ CO₂
– CO₂
HCO₃⁻·····H₂O